



# Sunflower trypsin inhibitor (SFTI-1) analogues of synthetic and biological origin via $N \rightarrow S$ acyl transfer: potential inhibitors of human Kallikrein-5 (KLK5)



Leila Shariff<sup>a</sup>, Yanan Zhu<sup>b</sup>, Ben Cowper<sup>a</sup>, Wei-Li Di<sup>b</sup>, Derek Macmillan<sup>a,\*</sup>

<sup>a</sup> Department of Chemistry, UCL, 20 Gordon Street, WC1H 0AJ, UK

<sup>b</sup> Institute of Child Health, UCL, 30 Guilford Street, London WC1N 1EH, UK

## ARTICLE INFO

### Article history:

Received 7 May 2014

Received in revised form 5 June 2014

Accepted 17 June 2014

Available online 20 June 2014

### Keywords:

Sunflower trypsin inhibitor

Native chemical ligation

KLK5

Atopic dermatitis

## ABSTRACT

Sunflower Trypsin Inhibitor (SFTI-1) analogues have been prepared from simple linear precursors produced either by chemical synthesis or following purification from *Escherichia coli*. We have shown, for the first time that these linear SFTI-1 derived peptide sequences can be converted to circular peptides via selective consecutive acyl transfer reactions, and that the products derived from synthetic and bacterial origin are identical. Preliminary analysis of the semi-synthetic SFTI-1 analogues confirmed SFTI-110H as an inhibitor of Kallikrein-5 (KLK5) protease that could also mediate its action on human keratinocytes. The preliminary results obtained serve as a useful starting point for the biological production of SFTI-1 based, selective KLK5 inhibitors for the treatment of atopic dermatitis.

© 2014 The Authors. Published by Elsevier Ltd. This is an open access article under the CC BY license (<http://creativecommons.org/licenses/by/3.0/>).

## 1. Introduction

Proteases are a diverse, ubiquitous class of enzymes that perform vital roles in a myriad of biological processes, such as apoptosis, blood coagulation and pathogenesis.<sup>1</sup> Protease inhibitors are key regulators of such processes, and therefore are extremely important pharmacological candidates. A number of therapeutic protease inhibitors are already available for clinical use, combating HIV/AIDS, cancer and hypertension, whilst proteases were recently estimated to represent 5–10% of current pharmaceutical targets.<sup>1,2</sup> This demonstrates a requirement for identification and development of new protease inhibitors.

The Bowman–Birk protein family is a group of approximately 50 serine protease inhibitors, found primarily in the seeds of plant species, where they are involved in protection of the host against pests and pathogens.<sup>3</sup> Bowman–Birk inhibitors (BBIs) typically comprise 60–90 amino acids, and perform dual inhibition of trypsin- and/or chymotrypsin-like proteases via disulfide-bonded  $\beta$ -hairpin loop motifs, which bind at catalytic sites via canonical protease recognition sequences.<sup>4,5</sup> In the early 1990s it was demonstrated that synthetic peptide mimics of the BBI  $\beta$ -hairpin loop motif retain biological activity.<sup>5,6</sup> Subsequently a naturally-

occurring  $\beta$ -hairpin peptide with broad inhibitory activity towards serine proteases was isolated from *Helianthus annuus* sunflower seeds.<sup>7</sup> Sunflower trypsin inhibitor-1 (SFTI-1) contains just 14 amino acids, including a disulfide bond and a contiguous circular peptide backbone. These features are not uncommon in small antimicrobial peptides,<sup>8</sup> conferring high rigidity and, consequently, potent activity; SFTI-1 is a significantly more potent inhibitor of bovine  $\beta$ -trypsin than BBIs and synthetic analogues.<sup>7</sup> Due to its size, stability and activity towards a range of proteases, SFTI-1 is an attractive therapeutic drug candidate, and has emerged recently as a useful framework for peptide ‘grafting’.<sup>9</sup> Mutation of selected SFTI-1 residues has improved selectivity towards certain substrates,<sup>10,11</sup> whilst insertion of bioactive peptide sequences into this circular scaffold has been shown to improve their in vivo stability.<sup>12</sup>

SFTI-1 is known to act upon a range of serine proteases, including cathepsin G7, matriptase,<sup>13</sup> and kallikrein-related peptidases (KLKs),<sup>14</sup> a group of fifteen related human proteases with roles in a variety of physiological processes and strong links to cancer progression.<sup>15,16</sup> Swedberg and co-workers recently observed inhibition of KLK4, a promising target for prostate cancer treatment, by SFTI-1.<sup>14</sup> They produced a sequence variant (where RCTK was modified to FCQR) with increased potency and improved selectivity over other proteases. Of the various proteases tested, the closely-related KLK5, itself implicated in prostate cancer progression<sup>17</sup> and skin conditions such as rosacea and atopic dermatitis,<sup>18,19</sup> exhibited comparatively weak inhibition by the

\* Corresponding author. Tel.: +44 020 7679 4684; e-mail address: [d.macmillan@ucl.ac.uk](mailto:d.macmillan@ucl.ac.uk) (D. Macmillan).

SFTI(FCQR) variant. Nonetheless this demonstrates the potential of the SFTI-1 framework as an inhibitor of KLK5. We have therefore sought to clarify the inhibitory activity of SFTI-1 derived peptides towards KLK5 (Fig. 1), with a view to studying its role in skin barrier homeostasis and developing selective therapeutic agents for the treatment atopic dermatitis.

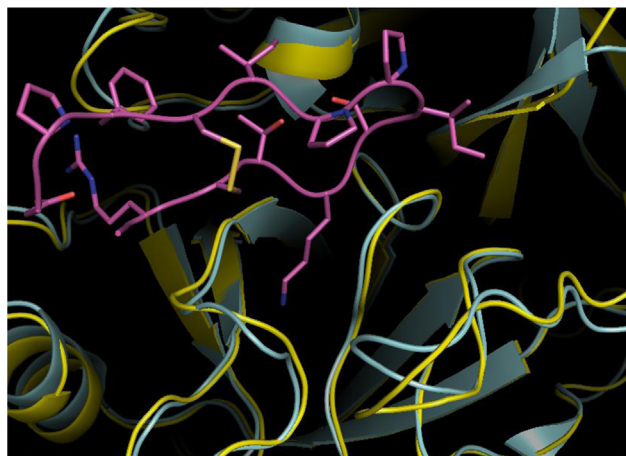


**Fig. 1.** Overlay of the SFTI-1/Trypsin complex (PDB ID: 1SFI) and KLK5 (PDB ID: 2PSX) emphasises the similarity between the structures around the SFTI-1 (magenta) binding site.

Numerous strategies are available for circular peptide production, involving both chemical<sup>20–22</sup> and biological<sup>23</sup> methods. We have recently demonstrated that circular peptides can be prepared in one-pot from a linear precursor adorned simply with a C-terminal Xaa-Cys motif (where Xaa preferably denotes Cys/His/Gly), which undergoes N→S acyl shift, and an N-terminal Cys, which intercepts a transient C-terminal thioester.<sup>24</sup> The peptide is ultimately cyclised via a native chemical ligation-type process.<sup>25</sup> Although several N→S acyl transfer methods have been reported,<sup>26</sup> this reaction can be routinely applied to linear peptides of synthetic or recombinant origin, with the requirement for only native amino acids facilitating bacterial protein expression, providing an alternative route to intein-mediated splicing strategies.<sup>27</sup> Here, we have utilised this strategy for the first time to produce both synthetic and recombinant analogues of SFTI-1, and demonstrated that the peptide is an inhibitor of KLK5 action on human keratinocytes in cell culture.

## 2. Results and discussion

Wild-type SFTI-1 is expressed as a fusion protein, embedded within seed storage albumin precursors (Fig. 2a), which are processed by an asparaginyl endopeptidase to cyclise the excised sequence.<sup>28</sup> For our purposes, in order to suitably position an Xaa-Cys motif at the C-terminus, the sequence was redesigned such that thioester formation could take place at this site (Fig. 2b, c). Neither of the native Arg-Cys nor Ile-Cys motifs were ideal for thioester synthesis via our N→S acyl transfer method and so Ile10 was initially substituted for glycine in model experiments (I10G). This substitution had previously been shown to give rise to a folded SFTI-1 analogue.<sup>10</sup> The linear SFTI-I10G precursor (Fig. 2b) could be readily prepared by automated solid phase peptide synthesis (SPPS) and by purification from *E. coli* as a fusion with thioredoxin. While solid phase synthesis of short circular peptides such as SFTI-analogues and cyclotides can be routinely achieved through total synthesis, the availability of a straightforward recombinant

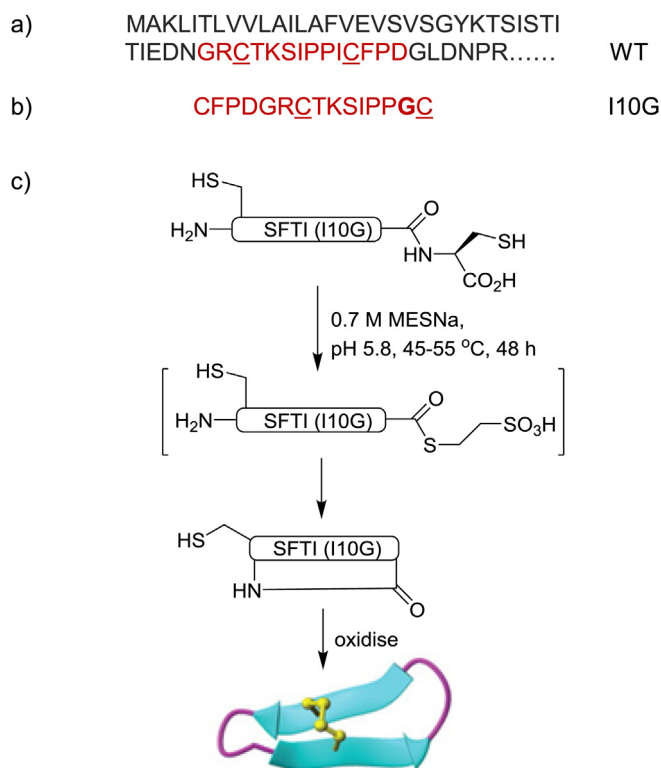


**Fig. 2.** Semi-synthesis of SFTI-1 analogues. (a) SFTI-1 Pro-peptide sequence with SFTI-1 shown in red. (b) Redesigned SFTI-1 derived sequence to enable cyclisation via N→S acyl transfer. (c) General reaction scheme for production of SFTI-1 analogues.

biological method renders thousands of analogues of these species available through straightforward DNA engineering. Biological production of the linear precursor also negates the need for wasteful use of organic solvents, excess building blocks, coupling reagents, protecting groups and proprietary linkers or solid supports.

Additionally our semi-synthetic method complements the few existing methods for the biological production of head-to-tail cyclic peptides such as intein- or sortase-mediated protein cyclisation and offers some advantages in that the expressed fusion protein need not be soluble or folded in order to be processed into cyclic product.

Synthetic SFTI-I10G was first prepared using Fmoc SPPS in automated fashion on commercially available Fmoc-Cys(Trt)-NovaSyn-TGT resin. After cleavage from the resin (95% v/v trifluoroacetic acid: 2.5% v/v H<sub>2</sub>O: 2.5% v/v 1,2-ethanedithiol) and HPLC purification the peptide was cyclised under typical reaction conditions.<sup>24,27</sup> This involved heating the sample, at an approximate concentration of 1 mg ml<sup>-1</sup> (0.5–1 mM) in 0.1 M sodium phosphate buffer; pH 5.8, to 55 °C in the presence of 10% w/v (0.7 M) sodium 2-mercaptoethane sulfonate (MESNa) for 48 h. After this time the cyclic peptide was recovered in 46% yield. In order to oxidise the resulting dithiol to the disulfide the peptide was stirred overnight in 0.1 M NaHCO<sub>3</sub> (pH 8.0) and the SFTI-1 analogue was then obtained after HPLC-purification.

For bacterial production of SFTI-I10G the *E. Coli* codon optimised DNA sequence, corresponding to the peptide shown in Fig. 2b, was purchased and cloned into expression vector pET 32a. The fusion was designed such that the desired linear precursor sequence would be expressed as an N-terminal fusion with His<sub>6</sub>-tagged thioredoxin, and released from the fusion protein following incubation with Tobacco Etch Virus (TEV) protease. Consequently the N-terminal Cys residue was preceded by the sequence ENLYFQ. The

fusion protein was over-expressed in BL21(DE3) cells and readily obtained from the soluble fraction of the cell-free extract, following  $\text{Ni}^{2+}$  affinity chromatography (Fig. 3a). 70 mg of the fusion protein could be routinely isolated from 1 L of cell culture. Fractions containing the fusion protein were pooled and dialysed against 50 mM Tris-HCl; pH 8 buffer containing 100 mM NaCl, 1 mM DTT and 0.5 mM EDTA prior to incubation with TEV protease ( $0.1 \text{ mg ml}^{-1}$ ). Exposure of the precursor to TEV protease resulted in almost complete liberation of the linear peptide in 4 h (Fig. 3b), which was subsequently isolated by preparative reverse-phase HPLC. Recovery of  $\sim 3 \text{ mg}$  of linear peptide per litre of cell culture was routinely achieved in this un-optimised process.

Furthermore,  $^1\text{H}$  NMR analysis of synthetic and recombinant SFTI-I10H analogues, recorded at the same pH, (pH 4.5, Fig. 5a) confirmed that both samples were identical. Comparison of the CH- $\alpha$  protons, commonly used to confirm the folded state of analogues, also showed that the I10H analogue was folded similarly to native SFTI-1 (Fig. 5b).<sup>9</sup> This data was extremely encouraging and so we set out to confirm that these analogues would serve as inhibitors of commercially available KLK5.

First, we optimised a fluorescence-based assay for KLK5 activity employing commercially available KLK5 substrate Boc-Val-Pro-Arg-AMC (Sigma). From the assay we established a  $K_m$  value of  $0.45 \mu\text{M}$  for this substrate, which was in good agreement with the

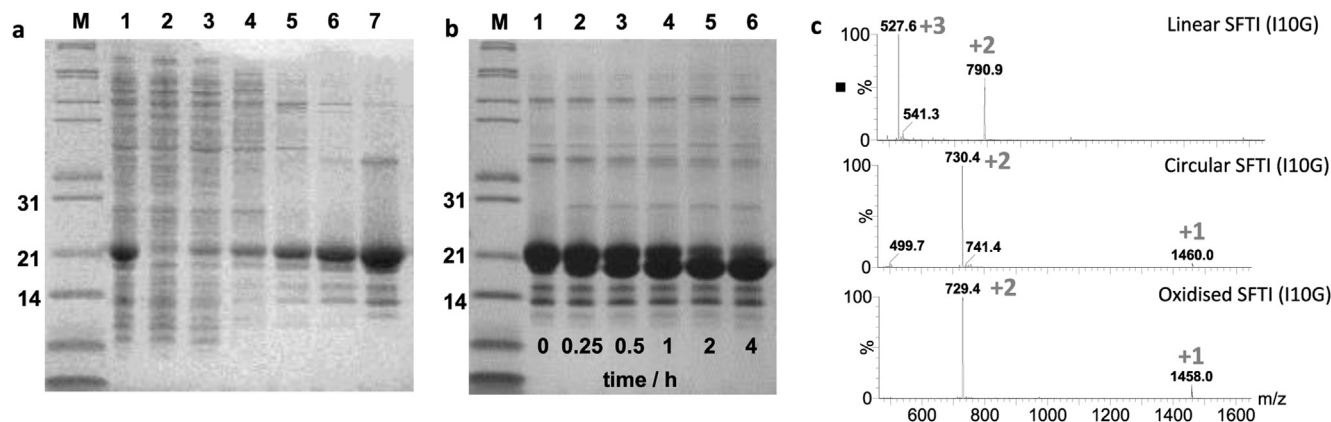


**Fig. 3.** (a) Purification of Trx-SFTI-I10G fusion protein. Lane M=molecular weight markers, lane 1=cell free extract (soluble fraction), lane 2=column flow-through, lanes 3–4=20 mM imidazole wash, lanes 5–7 40–250 mM imidazole elution. (b) TEV protease mediated cleavage of SFTI linear precursor from Trx. The SFTI peptide is too small to be visualised on the gel. (c) ESI-MS analysis of the HPLC purified linear precursor (upper panel), cyclised product (middle panel) and cyclised and oxidised SFTI analogue (bottom panel).

With the linear precursor in hand (Fig. 3c upper panel), the backbone was cyclised in a similar manner to that described above for the synthetic peptide (see experimental details for further information). The reaction was monitored by LC-MS, which clearly showed consumption of the starting material over a 48 h period at  $45^\circ\text{C}$ . The circular product (Fig. 3c, middle panel) was isolated by preparative HPLC and oxidised by stirring the sample in ammonium carbonate buffer overnight (Fig. 2c, lower panel). Both the synthetic and biological methods gave rise to sufficient quantities for examination of the structure and bioactivity. *E. coli* produced approximately  $250 \mu\text{g}$  of folded and oxidised peptide per litre of cell culture, which is comparable with intein-mediated methods.<sup>29</sup>

Although preliminary LC and MS analyses showed successful SFTI-I10G analogue synthesis we were concerned by the overly complex  $^1\text{H}$  NMR spectrum for the I10G analogue (Fig. 4a). While the signals corresponding to the folded peptide could be clearly observed through examination of the  $^1\text{H}$ - $^1\text{H}$  COSY, TOCSY, and NOESY spectra (see Supplementary data) there was clear evidence that this analogue existed in more than one significantly populated conformation. We presumed that removal of the side-chain of the native Ile10 residue in our I10G analogue was key to the increased conformational flexibility and so we prepared an I10H analogue (very amenable to  $N \rightarrow S$  acyl shift), to restore the steric bulk of the side-chain. Recombinant SFTI-I10H was prepared by site directed mutagenesis of the I10G template and both the recombinant and synthetic SFTI-I10H analogues were produced in an identical manner to their I10G counterparts, with near identical yields for each step. However, and in stark contrast to SFTI-I10G, SFTI-I10H gave rise to a simpler  $^1\text{H}$  NMR spectrum with sharp, well defined signals (Fig. 4b) suggesting the existence of a single preferred conformation in the folded structure.

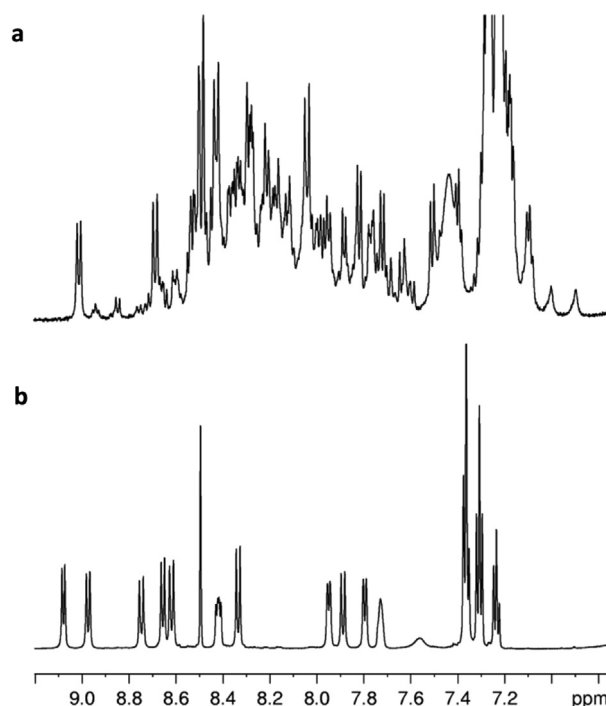


**Fig. 4.**  $^1\text{H}$  NMR analysis of the amide region of (a) SFTI-I10G, and (b) SFTI-I10H analogues.

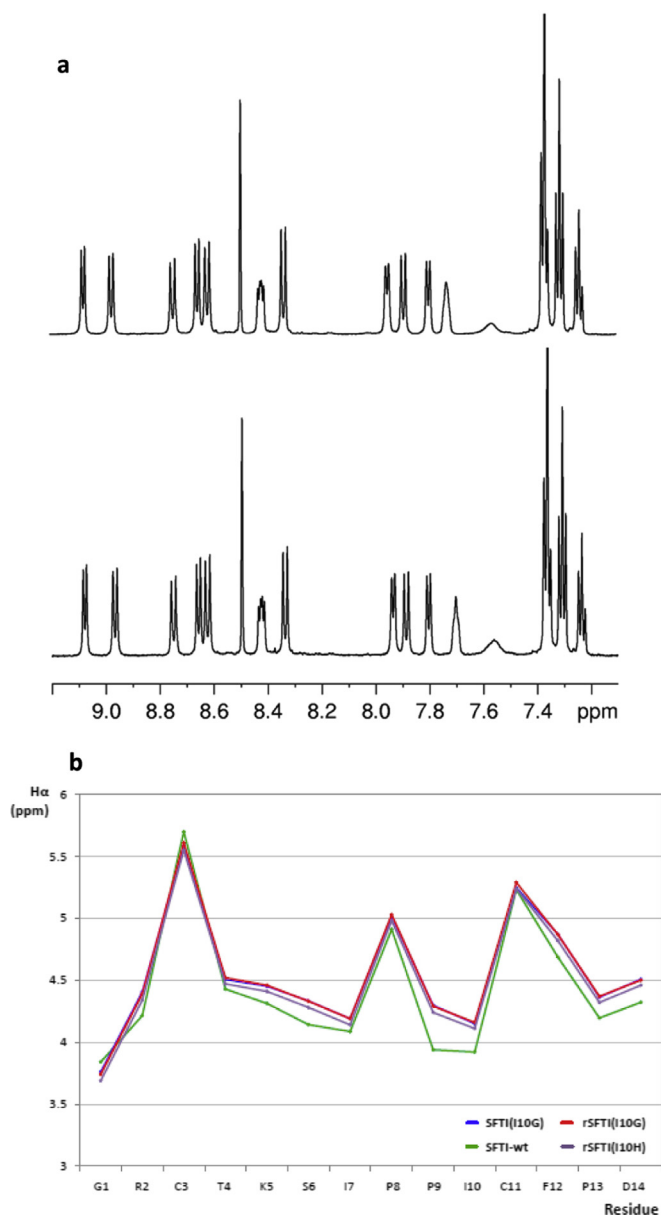


**Fig. 5.** (a)  $^1\text{H}$  NMR analysis of the amide region of the synthetic (upper spectrum) and bacterially-derived (lower spectrum) SFTI-I10H analogues. (b) Comparison of  $\text{CH}-\alpha$  proton chemical shifts for WT,<sup>10</sup> synthetic and recombinant I10G, and I10H analogues.

published value for this substrate ( $0.2 \mu\text{M}$ ).<sup>30</sup> Incubation of KLK5 and the 7-amido-4-methylcoumarin (AMC) substrate with increasing concentrations of SFTI analogues allowed preliminary  $\text{IC}_{50}$  data to be obtained (Table 1). As expected both analogues were found to inhibit KLK5 and the I10H analogue proved to be more than 100 times more active than the initial I10G analogue. An additional I10G analogue, where the Pro-Arg motif from the Boc-Val-

**Table 1**  
KLK5  $\text{IC}_{50}$  values for SFTI analogues

Entry	Peptide	$\text{IC}_{50}/\mu\text{M}$
1	SFTI-I10G	15.7
2	SFTI-I10G graft <sup>a</sup>	12.3
3	SFTI-I10H	0.14

<sup>a</sup> SFTI-I10G where CTK is replaced with sequence CPR.

Pro-Arg-AMC substrate substituted residues Thr-4 and Lys-5, was also prepared but showed little advantage in terms of inhibitory activity relative to the native sequence.

To further examine the KLK5 inhibitory activity of these SFTI analogues, a cell culture assay was performed. This assay relied on the known activation of protease activated receptor-2 (PAR-2), present on the surface of normal human keratinocytes, by KLK5. Proteolysis of PAR-2 by KLK5 results in exposure of a tethered ligand, which activates the receptor, triggering a pro-inflammatory intracellular G-protein-coupled pathway.<sup>18</sup> This process can be observed by measuring the temporary  $\text{Ca}^{2+}$  influx increase, which occurs as a result of PAR-2 activation by KLK5. The assay was performed by incubating the cells with KLK5 and increasing concentrations of SFTI analogue. The results (Fig. 6) showed that activation of PAR-2 was completely suppressed by  $50 \mu\text{M}$  SFTI-I10G or  $25 \mu\text{M}$  SFTI-I10H.

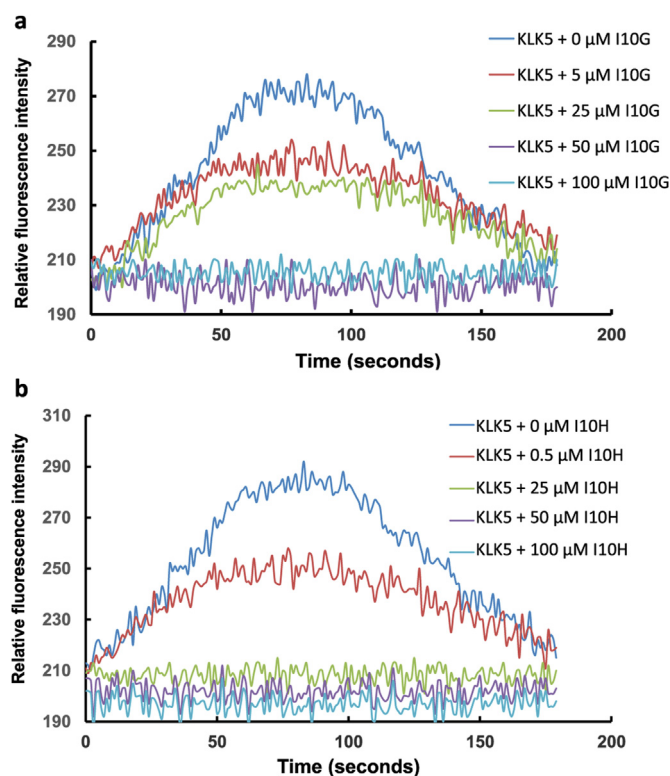


**Fig. 6.** Exposure of cultured human keratinocytes to recombinant KLK5 (100 ng) in the presence of (a) increasing SFTI-I10G and (b) SFTI-I10H analogues results in decreased  $\text{Ca}^{2+}$  influx.

### 3. Conclusion

In this study we have shown that Sunflower Trypsin Inhibitor (SFTI-1) analogues are readily available through either synthetic or biological means, from simple linear precursors, by  $N \rightarrow S$  acyl transfer followed by spontaneous cyclisation through native chemical ligation. The cyclic synthetic and bacterially derived products are identical.  $^1\text{H}$  NMR analysis also confirmed that, in contrast to the I10G analogue, SFTI-I10H adopts a single preferred conformation, perhaps emphasising the importance of the steric bulk associated with the side chain of this residue. While chemical synthesis offers advantages of simple incorporation of various amino acid analogues, the biological approach is easily scaled, less wasteful, ideal for library production through mutagenesis, and only requires water as solvent. Perhaps unsurprisingly (Fig. 1) both



I10G and I10H analogues were found to be KLK5 inhibitors *in vitro*. I10H was determined to have an  $IC_{50}$  of 0.14  $\mu$ M and the increased activity of SFTI-I10H over I10G was confirmed in human keratinocytes. The results serve as a useful starting point for the development of more potent and selective KLK5 inhibitory peptides, based on the SFTI scaffold.

## 4. Experimental section

### 4.1. General experimental details

Reversed-phase high performance liquid chromatography (RP-HPLC) was performed using a Dionex Ultimate 3000 system equipped with a Phenomenex Jupiter 10 $\mu$  Proteo 90A, C<sub>12</sub>, 250 $\times$ 21.2 mm column. Separations involved a mobile phase of 0.1% TFA (v/v) in water (solvent A)/acetonitrile (solvent B) over a 5–60% acetonitrile gradient. Analytical LC-MS was performed using a Waters Acquity UPLC SQD instrument equipped with an Acquity UPLC BEH, C<sub>18</sub>, 2.1  $\times$  50 mm column. Separations involved a mobile phase of 0.1% formic acid (v/v) in water (solvent A)/acetonitrile (solvent B) over a 5–95% acetonitrile gradient. For SDS-PAGE samples were denatured via addition to an equal volume of 2 $\times$  Laemmli loading buffer (containing 10 mM DTT) and incubation at 95 °C for 2 min. Samples were loaded onto 14% bis-Tris polyacrylamide gels, alongside Mark12 molecular weight marker (Invitrogen). Gels were run at 175 V using Novex XCell Sure-Lock apparatus (Invitrogen) and stained using Instant Blue (Triple Red).

### 4.2. Automated peptide synthesis

Automated solid-phase peptide synthesis (SPPS) was carried out on an ABI 433A automated synthesiser using standard Fmoc amino acids on a 0.05 mmol scale, and employing pre-loaded Fmoc-Cys(Trt)-NovaSyn<sup>®</sup>TGT resin (loading=0.19 mmol g<sup>-1</sup>). Cleavage of the assembled peptide chain was carried out in TFA (95% v/v)/1,2-ethanedithiol (2.5%)/H<sub>2</sub>O(2.5%) for 4.5 h before filtration and two cycles of precipitation into cold ether followed by centrifugation (4000 rpm, 4 °C, 15 min). Preparative RP-HPLC was performed with acetonitrile (0.1% v/v TFA) on a gradient of 5 $\rightarrow$ 60% (over 51 min, 7 mL min<sup>-1</sup>) and monitored at wavelengths 230 nm, 254 nm, and 280 nm.

### 4.3. Peptide cyclisation and oxidation

Linear precursors to SFTI-I10X analogues (where X=G or H) were assembled and purified as described above. HPLC fractions containing the desired peptide were identified by LC-MS and lyophilised. Backbone cyclisation was then carried out in sodium phosphate buffer (pH 5.8, 0.1 M) containing peptide (1 mg mL<sup>-1</sup>), sodium 2-mercaptoethane sulfonate (10% w/v) and sodium ascorbate (0.5% w/v). The samples were heated at 55 °C in an Eppendorf thermomixer with agitation (600 rpm) for 24 h. HPLC purification, as described above, yielded white powdered solids in 25–50% isolated yields. Finally, stirring of the cyclic peptides (0.1 mg mL<sup>-1</sup>) in 0.1 M ammonium bicarbonate solution (pH 8.0) at room temperature for 24 h yielded the disulfide-bonded structures. The reaction mixture was lyophilised, dissolved in the minimum volume of water and purified by RP-HPLC. Fractions containing the oxidised peptide were identified by LC-MS, pooled, and lyophilised to afford the target products in 80–100% yields.

### 4.4. Production of recombinant SFTI-1 analogues

The DNA sequence, codon optimised for *E. coli* expression, encoding the desired SFTI-I10G sequence preceded by cysteine-terminated TEV protease recognition site

(ENLYFQCFPDGRCTKSIPPGC-Stop), cloned into pUC57 vector, was purchased from Genscript. Flanking sequences 5'ggattgagggtcgcg (upstream) and 5'ggctctaactctctct (downstream) were incorporated to facilitate PCR amplification of the target insert, and cloning into the pET32 Xa/LIC vector (Invitrogen), according to manufacturers' instructions.

Thioredoxin(Trx)-SFTI fusion protein was expressed in *E. coli* BL21 (DE3) cells, via IPTG induction (1 mM final concentration) at O.D<sub>600</sub> ~0.6 followed by incubation at 30 °C for 3 h. Cells were harvested by centrifugation, resuspended in lysis buffer (20 mM Tris-HCl pH 7.9, 500 mM NaCl, 5 mM imidazole) supplemented with a complete protease inhibitor cocktail tablet (Roche) and 1 mM PMSF, before lysis via sonication for a net time period of 2 min. Soluble Trx-SFTI was purified by immobilised metal-ion chromatography (IMAC), analysed via SDS-PAGE, using Ni-IDA resin (Genscript), with washing and elution steps carried out using lysis buffer containing 30 mM and 200 mM imidazole, respectively. Eluted protein was dialysed overnight against 4 L TEV protease reaction buffer (50 mM Tris-HCl pH 8, 100 mM NaCl), and supplemented with DTT (1 mM) and EDTA (0.5 mM) before proteolysis by TEV protease (supplied by Dr Rachel Morgan, UCL) over four hours at 30 °C. The cleavage reaction was monitored by SDS-PAGE and LC-MS. Liberated linear SFTI peptide was purified via reversed-phase HPLC. Fractions containing the linear peptide were identified by LC-MS, pooled, and lyophilised.

A DNA expression construct encoding SFTI-I10H was created via site-directed mutagenesis, using SFTI-I10G-pET32 Xa/LIC as a template, primers 5'accaaaagcattccgccgcttgctaggcttaactc (forward) and 5'agtttagagccttagcaatgccgggaatgcttttgg (reverse), and a QuikChange II kit (Agilent) according to manufacturer's instructions. Protein expression, purification and proteolysis were carried out as described for SFTI-I10G.

### 4.5. Recombinant peptide cyclisation and folding

Backbone cyclisation reactions were carried out in a similar manner as for the synthetic samples. Briefly, lyophilised linear SFTI precursor peptides were dissolved in 0.1 M sodium phosphate pH 5.8 (1 mg/ml final concentration), containing MESNa (10% w/v) and TCEP (0.5% w/v) or sodium ascorbate (0.5% w/v). Reactions were agitated at 45 °C for 48 h, monitored via LC-MS, followed by purification via RP-HPLC. Oxidative folding was carried out via dissolution of peptides in 0.1 M ammonium bicarbonate pH 8.5 (0.1 mg/ml final concentration) followed by gentle stirring at room temperature for 24 h. Successful oxidation was verified via LC-MS, before purification of peptides via RP-HPLC.

### 4.6. NMR spectroscopy

NMR samples were constituted in 20 mM NaHPO<sub>4</sub> pH 4.5 supplemented with 10% D<sub>2</sub>O. <sup>1</sup>H, <sup>1</sup>H-<sup>1</sup>H COSY, <sup>1</sup>H-<sup>1</sup>H TOCSY and <sup>1</sup>H-<sup>1</sup>H NOESY spectra were acquired at 25 °C using 500 MHz, 600 MHz and 700 MHz Bruker Avance III spectrometers.

### 4.7. Protease inhibition assays

KLK 5 (0.5 mg mL<sup>-1</sup>, 0.63  $\mu$ L) was incubated for 3 min in reaction buffer: 50 mM Tris-HCl (pH 8.0) containing 20 mM CaCl<sub>2</sub> before addition of various concentrations of SFTI analogue (0.5 nM–66.2  $\mu$ M). Following further incubation (2 min), addition of fluorogenic Boc-VPR-AMC (79  $\mu$ M, 1.00  $\mu$ L) initiated the reaction, which was followed for 5 min on a Carey Eclipse fluorimeter (Agilent) set at excitation=380 nm and emission=460 nm. Blanks were performed without enzyme or inhibitor and controls without inhibitor. All reactions were performed in triplicate in a final reaction volume of approximately 150  $\mu$ L.

#### 4.8. Intracellular Ca<sup>2+</sup> analysis

Measurement of intracellular Ca<sup>2+</sup> flux was performed using the FluoForte™ Calcium Assay kit (Enzo Life Sciences). Human keratinocytes were plated in growth medium in 96-well plates at 1×10<sup>4</sup> cells/100 μL well. After 24 h, the growth medium was removed, and 100 μL of Dye-loading solution was added. The cells were further incubated for 45 min at 37 °C and 15 min at room temperature before stimulation, and during the incubation, 100 ng of recombinant human KLK5 was incubated with SFTI analogues at 37 °C for 10 min, after which the cells were challenged with the mixture of recombinant human KLK5 and SFTI analogue, and a time–response curve of intracellular [Ca<sup>2+</sup>] signal was recorded via real-time monitoring of fluorescence intensity at excitation=485 nm and emission=520 nm in a Microplate Reader (FLUOstar OPTIMA).

#### Acknowledgements

Authors acknowledge financial support from the UCL PhD programme in Drug Discovery and EPSRC.

#### Supplementary data

Supplementary data related to this article can be found at <http://dx.doi.org/10.1016/j.tet.2014.06.059>.

#### References and notes

- Turk, B. *Nat. Rev. Drug. Discovery* **2006**, *5*, 785–799.
- Drag, M.; Salvesen, G. S. *Nat. Rev. Drug. Discovery* **2010**, *9*, 690–701.
- Chilosi, G.; Caruso, C.; Caporale, C.; Leonardi, L.; Bertini, L.; Buzi, A.; Nobile, M.; Magro, P.; Buonocore, V. J. *Phytopathol.* **2000**, *148*, 477–481.
- Birk, Y. *Int. J. Pept. Protein Res.* **1985**, *25*, 113–131.
- Li, Y.; Huang, Q.; Zhang, S.; Liu, S.; Chi, C.; Tang, Y. J. *Biochem.* **1994**, *116*, 18–25.
- Domingo, G.; Leatherbarrow, R. J.; Freeman, N.; Patel, S.; Weir, M. *Int. J. Pept. Protein Res.* **1995**, *46*, 79–87.
- Lockett, S.; Garcia, R. S.; Barker, J. J.; Konarev, A. V.; Shewry, P. R.; Clarke, A. R.; Brady, R. L. *J. Mol. Biol.* **1999**, *290*, 525–533.
- Craik, D. J.; Allewell, N. M. *J. Biol. Chem.* **2012**, *287*, 26999–27000.
- Northfield, S. E.; Wang, C. K.; Schroeder, C. I.; Durek, T.; Kan, M.-W.; Swedberg, J. E.; Craik, D. J. *Eur. J. Med. Chem.* **2014**, *77*, 248–257.
- Quimbar, P.; Malik, U.; Sommerhoff, C. P.; Kaas, Q.; Chan, L. Y.; Huang, Y. H.; Grundhuber, M.; Dunse, K.; Craik, D. J.; Anderson, M. A.; Daly, N. L. *J. Biol. Chem.* **2013**, *288*, 13885–13896.
- Swedberg, J. E.; de Veer, S. J.; Sit, K. C.; Reboul, C. F.; Buckle, A. M.; Harris, J. M. *PLoS ONE* **2011**, *6*, e19302.
- Chan, L. Y.; Gunasekera, S.; Henriques, S. T.; Worth, N. F.; Le, S. J.; Clark, R. J.; Campbell, J. H.; Craik, D. J.; Daly, N. L. *Blood* **2011**, *118*, 6709–6717.
- Long, Y. Q.; Lee, S. L.; Lin, C. Y.; Enyedy, I. J.; Wang, S.; Li, P.; Dickson, R. B.; Roller, P. P. *Bioorg. Med. Chem. Lett.* **2001**, *11*, 2515–2519.
- Swedberg, J. E.; Nigon, L. V.; Reid, J. C.; de Veer, S. J.; Walpole, C. M.; Stephens, C. R.; Walsh, T. P.; Takayama, T. K.; Hooper, J. D.; Clements, J. A.; Buckle, A. M.; Harris, J. M. *Chem. Biol.* **2009**, *16*, 633–643.
- Emami, N.; Diamandis, E. P. *J. Biol. Chem.* **2008**, *283*, 3031–3041.
- Borgoño, C. A.; Diamandis, E. P. *Nat. Rev. Cancer* **2004**, *4*, 876–890.
- Michael, I. P.; Pampalakis, G.; Mikolajczyk, S. D.; Malm, J.; Sotiropoulou, G.; Diamandis, E. P. *J. Biol. Chem.* **2006**, *281*, 12743–12750.
- Briot, A.; Deraison, C.; Lacroix, M.; Bonnart, C.; Robin, A.; Besson, C.; Dubus, P.; Hovnanian, A. *J. Exp. Med.* **2009**, *206*, 1135–1147.
- Coda, A. B.; Hata, T.; Miller, J.; Audish, D.; Kotol, P.; Two, A.; Shafiq, F.; Yamasaki, K.; Harper, J. C.; Del Rosso, J. Q.; Gallo, R. L. *J. Am. Acad. Dermatol.* **2013**, *69*, 570–577.
- Zhang, L.; Tam, J. P. *J. Am. Chem. Soc.* **1997**, *119*, 2363–2370.
- Tam, J. P.; Wong, C. T. *J. Biol. Chem.* **2012**, *287*, 27020–27025.
- Zheng, J.-S.; Tang, S.; Guo, Y.; Chang, H.-N.; Liu, L. *ChemBioChem* **2012**, *13*, 542–546.
- Aboye, T. L.; Camarero, J. A. *J. Biol. Chem.* **2012**, *287*, 27026–27032.
- Macmillan, D.; De Cecco, M.; Reynolds, N. L.; Santos, L. F.; Barran, P. E.; Dorin, J. R. *ChemBioChem* **2011**, *12*, 2133–2136.
- Dawson, P. E.; Muir, T. W.; Clark-Lewis, I.; Kent, S. B. *Science* **1994**, *266*, 776–779.
- Macmillan, D.; Adams, A.; Premdjee, B. *Isr. J. Chem.* **2011**, *51*, 885–899.
- Cowper, B.; Craik, D. J.; Macmillan, D. *ChemBioChem* **2013**, *14*, 809–812.
- Mylyne, J. S.; Colgrave, M. L.; Daly, N. L.; Chanson, A. H.; Elliott, A. G.; McCallum, E.; Jones, A.; Craik, D. J. *Nat. Chem. Biol.* **2011**, *7*, 257–259.
- Austin, J.; Kimura, R. H.; Woo, Y.-H.; Camarero, J. A. *Amino Acids* **2010**, *38*, 1313–1322.
- Michael, I. P.; Sotiropoulou, G.; Pampalakis, G.; Magklara, A.; Ghosh, M.; Wasney, G.; Diamandis, E. P. *J. Biol. Chem.* **2005**, *15*, 14628–14635.